

Holon edge states in organic conductors (TMTTF)₂X in the charge-gap regime

Andrei V. Lopatin and Victor M. Yakovenko

Department of Physics and Center for Superconductivity Research, University of Maryland, College Park, MD 20742-4111
(cond-mat/0106516, June 25, 2001)

Using the bosonization technique, which separates charge and spin degrees of freedom, we study a possibility of formation of the holon edge states in a one-dimensional electron system with an energy gap in the charge sector. The results are applied to the quasi-one-dimensional organic conductors (TMTTF)₂X. The different roles of the bond and site dimerizations in this material are discussed. We predict that the holon edge states should appear below the temperature of the recently discovered ferroelectric transition, where the inorganic anions X displace to asymmetric positions.

When the bulk electron states have an energy gap, additional states may exist on the surface with the energies inside the gap. Such surface states were studied for a long time in the cases where the gap has a band-structure origin [1]. More recently, edge states attracted much interest in the cases where the gap originates from a phase transition in the electron system. Examples are midgap states in the high- T_c d -wave cuprate superconductors [2] and chiral states in the p -wave superconductor Sr₂RuO₄ (see, for example, Ref. [3] and references therein). Edge states in the quasi-one-dimensional (Q1D) organic conductors (TMTSF)₂X [4] were studied for the triplet superconducting state [5] and for the magnetic-field-induced spin-density-wave (FISDW) state [6], which exhibits the quantum Hall effect. In all of these cases, noninteracting electrons were subject to a mean-field potential, so the problem reduced to a single-particle Schrödinger-like equation with a boundary. However, it is known that a one-dimensional (1D) system of interacting electrons can be described in terms of separate charge and spin sectors (see, for example, review [7]). An edge state in such a system with a gap in the spin channel was studied in Ref. [8]. In this Letter, we use the technique developed in Ref. [8] (see also Ref. [9]) to investigate another physical situation where a gap opens in the charge sector. The charge gap appears when the electron system is commensurate with the crystal lattice, and the umklapp interaction becomes relevant. This is the case for the (TMTTF)₂X family of Q1D organic conductors [10], which are the best known examples of spin-charge separation. In these materials, electric transport is thermally-activated due to the charge gap, whereas spin susceptibility only weakly depends on temperature, which indicates gapless spin sector.

The (TMTTF)₂X crystals consist of parallel 1D molecular chains quarter-filled with holes. The umklapp term appears due to dimerization of the chains. Generally, there are two sources of dimerization, one due to nonequivalence of hopping integrals along the chain, and another due to nonequivalence of the site potentials. The unit cell consists of two organic molecules TMTTF and one inorganic anion X. The anions X are located outside of the TMTTF chain, between the pairs of TMTTF molecules, as shown in Fig. 1. Because of the anions, the bonds between the TMTTF molecules alternate between

short and long. At high temperatures, the anions occupy symmetric positions, so the TMTTF molecules themselves are equivalent. However, it was recently proved that below a certain transition temperature, the anions displace to asymmetric positions, making the two TMTTF molecules in a unit cell nonequivalent [11]. In this Letter, we show that one source of dimerization controls the existence and the localization length the edge states, whereas the other source determines their energy.

In our theoretical model, we neglect interchain coupling and consider just one semi-infinite chain. For simplicity, we will refer to holes as electrons and set $\hbar = 1$. The electron band structure of the chain is described by the Hamiltonian

$$\hat{H} = - \sum_{n=1, s}^{\infty} \left[t_n (\hat{\psi}_{n,s}^\dagger \hat{\psi}_{n+1,s} + \text{H.c.}) + \mu_n \hat{\psi}_{n,s}^\dagger \hat{\psi}_{n,s} \right], \quad (1)$$

$$t_n = t - (-1)^n \bar{t}/2, \quad \mu_n = \mu - (-1)^n \bar{\mu}, \quad (2)$$

where the index n labels the TMTTF sites, $s = \uparrow, \downarrow$ is the spin index, and $\hat{\psi}_{n,s}^{(\dagger)}$ are the creation and annihilation operators of electrons. The mean values of the intersite tunneling amplitude and the chemical potential are t and μ , whereas \bar{t} and $\bar{\mu}$ are their staggering parts produced by dimerization of the chain bonds and sites, respectively.

The energy dispersion for the Hamiltonian (1) and (2) is sketched in Fig. 2. For a given chemical potential μ , there exist two Fermi points $\pm k_F$. To study low-energy properties of the system, we introduce the operators \hat{R} and \hat{L} describing the right- and left-moving electrons with the momenta close to $+k_F$ and $-k_F$:

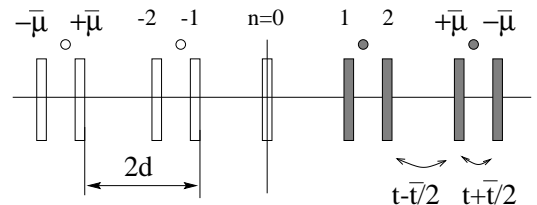


FIG. 1. A sketch of the (TMTTF)₂X chain. The vertical rectangles represent the organic molecules TMTTF, and the circles indicate the inorganic anions X. The filled objects ($n = 0, 1, \dots$) show the actual chain, whereas the open objects ($n = 0, -1, -2, \dots$) represent an artificial expansion of the system by the mirror reflection around the site $n = 0$.

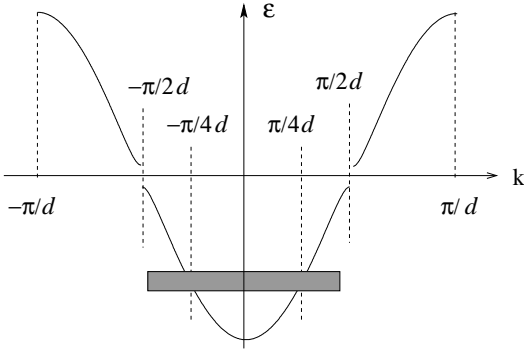


FIG. 2. The energy dispersion for the Hamiltonian (1). The single-particle gap at $k = \pm\pi/2d$ opens due to backscattering (5) caused by the chain dimerization (2). The correlation gap at $k = \pm\pi/4d$ is caused by umklapp interaction.

$$\hat{\psi}_s(x) = \left[e^{ik_F x} \hat{R}_s(x) - e^{-ik_F x} \hat{L}_s(x) \right] \sqrt{d}. \quad (3)$$

Here $x = nd$ is the continuous coordinate, and d is the average distance between the TMTTF sites.

The considered system (1) extends in the positive direction from the site $n = 1$ to a length l , which will be taken to infinity. The wave functions ψ_n can be expanded to include the site $n = 0$ with the vanishing boundary condition $\psi_0 = 0$. Then the system can be artificially expanded from the interval $(0, l)$ to $(-l, l)$ by the mirror reflection around the origin $n = 0$, as shown in Fig. 1, while keeping only the antisymmetric wave functions $\psi_n = -\psi_{-n}$. Because the Hamiltonian (1) couples only the nearest neighboring sites, such an expanded problem is equivalent to the original semi-infinite problem, because there is no direct coupling between the intervals $(-l, 0)$ and $(0, l)$ other than through the point $n = 0$, where the wave function vanishes. As Fig. 1 shows, the mirror reflection changes the sign of the bond dimerization parameter \bar{t} , but keeps the same sign for the site dimerization $\bar{\mu}$. Thus, for the expanded problem, Eq. (2) should be replaced by $t_n = t - \text{sgn}(n)(-1)^n \bar{t}$. In the continuous expanded system, the boundary condition $\hat{\psi}(0) = 0$ is satisfied by demanding that $\hat{\psi}(x) = -\hat{\psi}(-x)$. Using Eq. (3), the latter condition gives

$$\hat{R}(x) = \hat{L}(-x). \quad (4)$$

Dimerized chain at half filling. As a warm-up, let us study the edge states for noninteracting electrons at half filling, where $\mu = 0$ and $k_F = \pi/2d$ (see Fig. 2). Although the model (1) and (2) at half filling does not correspond to $(\text{TMTTF})_2\text{X}$, it does describe some 1D polymers [12], which have both site and bond dimerization. The nondimerized part of the Hamiltonian (1) is

$$\hat{H}_0 = \sum_s \int_0^l dx v_F \left[-\hat{R}_s^\dagger(x) i\partial_x \hat{R}_s(x) + \hat{L}_s^\dagger(x) i\partial_x \hat{L}_s(x) \right],$$

where $v_F = 2td$ is the Fermi velocity. The dimerized part of the Hamiltonian (1) gives the backscattering term:

$$\hat{H}_{\text{bs}} = \sum_s \int_0^l dx \left[(-\bar{\mu} + i\bar{t}) \hat{R}_s^\dagger(x) \hat{L}_s(x) + \text{H.c.} \right]. \quad (5)$$

The energies ε and the wave functions $R(x)$ and $L(x)$ of electron eigenstates can be found from the corresponding Schrödinger equation

$$\begin{pmatrix} -iv_F \partial_x & -\bar{\mu} + i\bar{t} \\ -\bar{\mu} - i\bar{t} & +iv_F \partial_x \end{pmatrix} \begin{pmatrix} R(x) \\ L(x) \end{pmatrix} = \varepsilon \begin{pmatrix} R(x) \\ L(x) \end{pmatrix}. \quad (6)$$

Eq. (6) gives the spectrum $\varepsilon = \sqrt{v_F^2 k^2 + \Delta^2}$ for the bulk states with the energy gap $\Delta = \sqrt{\bar{\mu}^2 + \bar{t}^2}$.

With the boundary condition $\psi(0) = 0$, which translates into $R(0) = L(0)$ using Eq. (3), Eq. (6) also gives a solution localized at the edge (the Shockley state [1]):

$$R_e(x) = L_e(x) = e^{-\kappa x}, \quad \varepsilon_e = -\bar{\mu}, \quad \kappa = -\bar{t}/v_F. \quad (7)$$

Eq. (7) shows that the energy of the edge state is determined by the site dimerization $\bar{\mu}$, whereas its localization length $1/\kappa$ by the bond dimerization \bar{t} . The edge state exists only when $\bar{t} < 0$, i.e. when the edge site ($n = 1$) is connected to the next site ($n = 2$) by the long bond. That configuration is opposite to what is drawn in Fig. 1, where the first bond is short.

Using Eq. (4), we get Eq. (6) in the expanded picture:

$$-i\partial_x R(x) - [\bar{\mu} - i\bar{t} \text{sgn}(x)] R(-x) = \varepsilon R(x). \quad (8)$$

The edge state (7) maps onto a state localized around the kink in the imaginary part of the potential in Eq. (8), which is produced by the sign change of the bond dimerization \bar{t} upon mirror reflection around $n = 0$. Such soliton states were studied for polymers in Ref. [12].

Quarter filling. In this case, $k_F = \pi/4d$, as shown in Fig. 2, and there is no single-particle energy gap at the Fermi level. However, a correlation gap (shown as the shaded bar in Fig. 2) may develop at the Fermi level due to interaction between electrons. Thus, we add the Hubbard interaction $U \sum_n \hat{\psi}_{n\uparrow}^\dagger \hat{\psi}_{n\downarrow}^\dagger \hat{\psi}_{n\downarrow} \hat{\psi}_{n\uparrow}$. It can be rewritten in the standard g -ology form [7] in terms of the slow fields \hat{R} and \hat{L} . Without dimerization, one obtains

$$\begin{aligned} \hat{H}_{\text{int}} = \sum_{s,s'} \int_0^l dx \left\{ 2(g_{1\parallel} \delta_{ss'} + g_{1\perp} \delta_{\bar{s}s'}) \hat{R}_s^\dagger \hat{L}_{s'}^\dagger \hat{R}_{s'} \hat{L}_s \right. \\ \left. + 2g_2 \hat{R}_s^\dagger \hat{L}_{s'}^\dagger \hat{L}_{s'} \hat{R}_s + g_4 [\hat{R}_s^\dagger \hat{R}_{s'}^\dagger \hat{R}_{s'} \hat{R}_s + (\hat{R} \rightarrow \hat{L})] \right\}, \quad (9) \end{aligned}$$

where $\bar{s} = \downarrow, \uparrow$ for $s = \uparrow, \downarrow$.

Introducing the densities of spin and charge

$$\hat{\rho}_R = \frac{\hat{R}_\uparrow^\dagger \hat{R}_\uparrow + \hat{R}_\downarrow^\dagger \hat{R}_\downarrow}{\sqrt{2}}, \quad \hat{\sigma}_R = \frac{\hat{R}_\uparrow^\dagger \hat{R}_\uparrow - \hat{R}_\downarrow^\dagger \hat{R}_\downarrow}{\sqrt{2}}, \quad (10)$$

the interaction Hamiltonian (9) can be written as

$$\hat{H}_{\text{int}} = \hat{H}_{\text{int}}^{(\sigma)} + \hat{H}_{\text{int}}^{(\rho)} + 2g_{1\perp} \sum_s \int_0^l dx \hat{R}_s^\dagger \hat{L}_s^\dagger \hat{R}_s \hat{L}_s, \quad (11)$$

$$\hat{H}_{\text{int}}^{(\rho)} = \int_0^l dx [g_4(\hat{\rho}_R^2 + \hat{\rho}_L^2) - 2g_5 \hat{\rho}_R \hat{\rho}_L], \quad (12)$$

$$\hat{H}_{\text{int}}^{(\sigma)} = - \int_0^l dx [g_4(\hat{\sigma}_R^2 + \hat{\sigma}_L^2) + 2g_{1\parallel} \hat{\sigma}_R \hat{\sigma}_L], \quad (13)$$

where $g_5 = g_{1\parallel} - 2g_2$.

The umklapp term. Taking into account that dimerization (2), treated as a perturbation, hybridizes the states with the momenta $k = \pm k_F = \pm\pi/4d$ and $k = \mp 3\pi/4d$, we make the following replacement in Eq. (3)

$$e^{\pm ik_F x} \longrightarrow e^{\pm i\pi n/4} - \frac{\bar{\mu} \pm i\bar{t}/\sqrt{2}}{\delta E} e^{\mp i3\pi n/4}, \quad (14)$$

where $\delta E = 2t\sqrt{2}$. Inserting Eqs. (3) and (14) into the Hubbard interaction term, we obtain the umklapp term

$$\hat{H}_{\text{um}} = \int_0^l dx [(g_3^a + ig_3^b) \hat{R}_\uparrow^\dagger \hat{R}_\downarrow^\dagger \hat{L}_\downarrow \hat{L}_\uparrow + \text{H.c.}], \quad (15)$$

$$g_3^a = -\sqrt{2}U\bar{\mu}d/t, \quad g_3^b = U\bar{t}d/t. \quad (16)$$

The real part g_3^a of the umklapp amplitude is proportional to the site dimerization energy $\bar{\mu}$, which occurs due to the anion displacement, and the imaginary part g_3^b is proportional to the bond dimerization \bar{t} .

Bosonization with a boundary. As Eq. (4) shows, the problem on the expanded interval $(-l, l)$ can be formulated in terms of the right-moving electrons only. The kinetic energy \hat{H}_0 becomes

$$\hat{H}_0 = -v_F \sum_s \int_{-l}^l dx \hat{R}_s^\dagger(x) i\partial_x \hat{R}_s(x), \quad (17)$$

where $v_F = td/\sqrt{2}$ for the quarter filling. Imposing the periodic boundary condition $\hat{R}(-l) = \hat{R}(l)$ together with Eq. (4) results in the vanishing boundary condition on $\hat{\psi}$ at the other end of the chain: $\hat{\psi}(l) = 0$. Now we can use the standard bosonization technique [7] for \hat{R} . The fermion fields $\hat{R}_s(x)$ can be represented in terms of the Bose fields $\hat{\theta}_s(x)$:

$$\hat{R}_s(x) = \hat{\eta}_s e^{i\hat{\theta}_s(x)} (2\pi\zeta)^{-1/2}, \quad (18)$$

where ζ is a short-range cut-off distance of the order of d , and $\hat{\eta}_s$ are the Majorana fermions: $\{\hat{\eta}_\uparrow, \hat{\eta}_\downarrow\} = 0$, $\hat{\eta}_s^2 = 1$. The Bose fields obey the commutation relations

$$[\hat{\theta}_s(x), \hat{\theta}_{s'}(x')] = i\pi \delta_{ss'} \text{sgn}(x - x'). \quad (19)$$

Using the linear combinations

$$\hat{\theta}_\rho = (\hat{\theta}_\uparrow + \hat{\theta}_\downarrow)/\sqrt{2}, \quad \hat{\theta}_\sigma = (\hat{\theta}_\uparrow - \hat{\theta}_\downarrow)/\sqrt{2}, \quad (20)$$

the charge and spin densities (10), can be expressed in terms of the charge and spin Bose fields (20):

$$\hat{\rho}_R(x) = \partial_x \hat{\theta}_\rho(x)/2\pi, \quad \hat{\sigma}_R(x) = \partial_x \hat{\theta}_\sigma(x)/2\pi. \quad (21)$$

The Hamiltonian (17) can be rewritten in terms of the densities (21) [7]:

$$\hat{H}_0 = \pi v_F \int_{-l}^l dx [\hat{\rho}_R^2(x) + \hat{\sigma}_R^2(x)]. \quad (22)$$

Substituting Eqs. (4) and (18) into the interaction Hamiltonian (11) and (15) and adding the kinetic energy (22), we get the full Hamiltonian of the system in the bosonized form. It takes the form $\hat{H}_\rho + \hat{H}_\sigma$, where the spin and charge sectors are separated. The charge Hamiltonian is

$$\hat{H}_\rho = \int_{-l}^l dx [\pi v_\rho \hat{\rho}_R^2(x) - g_5 \hat{\rho}_R(x) \hat{\rho}_R(-x) - \frac{g_3^a + ig_3^b \text{sgn}(x)}{(2\pi\zeta)^2} e^{-i\sqrt{2}[\hat{\theta}_\rho(x) - \hat{\theta}_\rho(-x)]}]. \quad (23)$$

Notice that the imaginary part of the umklapp amplitude in Eq. (23) has a kink, because it is proportional to \bar{t} (16), which changes sign between $x < 0$ and $x > 0$. The spin Hamiltonian is

$$\hat{H}_\sigma = \int_{-l}^l dx [\pi v_\sigma \hat{\sigma}_R^2(x) - g_{1\parallel} \hat{\sigma}_R(x) \hat{\sigma}_R(-x) + \frac{2g_{1\perp}}{(2\pi\zeta)^2} e^{-i\sqrt{2}[\hat{\theta}_\sigma(x) - \hat{\theta}_\sigma(-x)]}]. \quad (24)$$

In Eqs. (23) and (24), $v_{\rho,\sigma} = v_F \pm g_4/\pi$.

The quadratic parts of the Hamiltonians (23) and (24) can be diagonalized by the Bogoliubov transformations

$$\hat{\theta}_{\rho,\sigma}(x) = \tilde{\theta}_{\rho,\sigma}(x) \cosh \phi_{\rho,\sigma} - \tilde{\theta}_{\rho,\sigma}(-x) \sinh \phi_{\rho,\sigma}, \quad (25)$$

$$\hat{\rho}_R(x) = \tilde{\rho}(x) \cosh \phi_\rho + \tilde{\rho}(-x) \sinh \phi_\rho, \quad (26)$$

$$\hat{\sigma}_R(x) = \tilde{\sigma}(x) \cosh \phi_\sigma + \tilde{\sigma}(-x) \sinh \phi_\sigma, \quad (27)$$

where $\tanh 2\phi_\rho = g_5/\pi v_\rho$ and $\tanh 2\phi_\sigma = g_{1\parallel}/\pi v_\sigma$. The charge Hamiltonian becomes

$$\hat{H}_\rho = \int_{-l}^l dx [\pi \tilde{v}_\rho (\partial_x \tilde{\theta}_\rho(x)/2\pi)^2 - \frac{g_3^a + ig_3^b \text{sgn}(x)}{(2\pi\zeta)^2} e^{-i\sqrt{2K_\rho}[\tilde{\theta}_\rho(x) - \tilde{\theta}_\rho(-x)]}], \quad (28)$$

where $\tilde{v}_\rho = v_\rho/\cosh 2\phi_\rho$ and $K_\rho = e^{2\phi_\rho}$. Similarly, for the spin Hamiltonian, we get

$$\hat{H}_\sigma = \int_{-l}^l dx [\pi \tilde{v}_\sigma (\partial_x \tilde{\theta}_\sigma(x)/2\pi)^2 + \frac{2g_{1\perp}}{(2\pi\zeta)^2} e^{-i\sqrt{2K_\sigma}[\tilde{\theta}_\sigma(x) - \tilde{\theta}_\sigma(-x)]}], \quad (29)$$

where $\tilde{v}_\sigma = v_\sigma/\cosh 2\phi_\sigma$ and $K_\sigma = e^{2\phi_\sigma}$.

The umklapp term [the last term in Eq. (28)] is irrelevant when $K_\rho > 1$ [7]. In the opposite case $K_\rho < 1$, this

term is relevant and leads to opening of an energy gap in the charge sector. At the particular value $K_\rho = 1/2$, the charge Hamiltonian \hat{H}_ρ can be mapped to a model of noninteracting fermions with an energy gap [7,13]. By introducing the effective fermions (holons)

$$\tilde{\psi}_\rho(x) = e^{i\tilde{\theta}_\rho(x)} (2\pi\zeta)^{-1/2}, \quad (30)$$

and taking into account the commutation relations (19), the last term in Eq. (28) can be written as

$$\frac{e^{-i[\tilde{\theta}_\rho(x) - \tilde{\theta}_\rho(-x)]}}{(2\pi\zeta)^2} = -i \text{sign}(x) \frac{\tilde{\psi}_\rho^\dagger(x) \tilde{\psi}_\rho(-x)}{2\pi\zeta}. \quad (31)$$

Then the charge Hamiltonian (28) becomes

$$\begin{aligned} \hat{H}_\rho = & \int_{-l}^l dx \left\{ -\tilde{v}_\rho \tilde{\psi}_\rho^\dagger(x) i \partial_x \tilde{\psi}_\rho(x) \right. \\ & \left. - [g_3^b - i g_3^a \text{sgn}(x)] \tilde{\psi}_\rho^\dagger(x) \tilde{\psi}_\rho(-x) / 2\pi\zeta \right\}. \quad (32) \end{aligned}$$

The energy spectrum ε_ρ of the Hamiltonian (32) can be found from the corresponding Schrödinger equation

$$-i\tilde{v}_\rho \partial_x \tilde{\psi}_\rho(x) - \frac{g_3^b - i g_3^a \text{sgn}(x)}{2\pi\zeta} \tilde{\psi}_\rho(-x) = \varepsilon_\rho \tilde{\psi}_\rho(x). \quad (33)$$

Eq. (33) is formally equivalent to Eq. (8) with g_3^b and g_3^a playing the roles of $\bar{\mu}$ and \bar{t} , respectively. However, as Eq. (16) shows, $g_3^b \propto \bar{t}$ and $g_3^a \propto \bar{\mu}$, so the roles of $\bar{\mu}$ and \bar{t} are reversed in Eq. (33) compared with Eq. (8). This is a consequence of the factor $-i \text{sign}(x)$ in Eq. (31). Eq. (33) gives the spectrum $\varepsilon_\rho = \sqrt{\tilde{v}_\rho^2 k^2 + \Delta_\rho^2}$ for the bulk states with the charge gap $\Delta_\rho = \sqrt{(g_3^b)^2 + (g_3^a)^2} / 2\pi\zeta$. It also gives an edge solution localized around $x = 0$:

$$\tilde{\psi}_{\rho e}(x) = e^{-\kappa|x|}, \quad (34)$$

$$\varepsilon_{\rho e} = -g_3^b / 2\pi\zeta = -\Delta_\rho \bar{t} / \sqrt{\bar{t}^2 + 2\bar{\mu}^2}, \quad (35)$$

$$\kappa = -g_3^a / 2\pi\zeta \tilde{v}_\rho = (\Delta_\rho / \tilde{v}_\rho) \bar{\mu} / \sqrt{\bar{\mu}^2 + \bar{t}^2 / 2}, \quad (36)$$

where we used Eq. (16) assuming $U > 0$ for the repulsive Hubbard model. We see that, opposite to the electron edge state (7), the energy (35) of the holon edge state (34) is determined by the bond dimerization \bar{t} and its localization length (36) is controlled by the site dimerization $\bar{\mu}$. The holon edge state exists only when $g_3^a < 0$, i.e. $\bar{\mu} > 0$. Taking into account Eq. (2), we conclude that the holon edge state exists when the chemical potential of the edge site ($n = 1$) is higher, i.e. when the anion displaces toward the edge site, as shown in Fig. 1. Thus, we predict that the holon edge states should appear in (TMTTF)₂X below the anion transition temperature [11]. Their energies (35) depend on whether the first bond at the edge is short or long.

Similar consideration [8] can be done for the spin Hamiltonian (29). A gap in the spin sector opens when

$K_\sigma < 1$, i.e. $g_{1\parallel} < 0$ [7], whereas the required condition for the existence of an edge state is $g_{1\perp} > 0$. However, $g_{1\perp} = g_{1\parallel}$ in a physical system because of the spin SU(2) invariance. So, it is not possible to satisfy the conditions for opening of a gap and existence of an edge state simultaneously. Thus, we conclude, contrary to Ref. [8], that spinon edge states cannot exist.

In conclusion, we have shown that holon edge states may appear in a 1D model of interacting electrons with an energy gap in the charge sector. The existence of the holon edge state and its localization length are controlled by the real part of the umklapp interaction amplitude, whereas its energy is determined by the imaginary part. In the quasi-one-dimensional organic conductors (TMTTF)₂X, these umklapp amplitudes are proportional to the site and bond dimerizations, correspondingly. The bond dimerization is always present in these materials. However, the site dimerization occurs only below the recently discovered ferroelectric transition, where the inorganic anions X displace to asymmetric positions [11]. We predict that the holon edge states should appear below the anion transition. They could be probed by electron tunneling into the ends of 1D chains or by other types of spectroscopy.

V.M.Y. is grateful to K. Le Hur and S. A. Brazovskii for drawing his attention to Refs. [8,9] and [11] respectively. This work was supported by the Packard Foundation and NSF Grant No. DMR-9815094.

-
- [1] S. G. Davison and M. Stęślička, *Basic Theory of Surface States* (Oxford University Press, Oxford, 1996).
 - [2] C.-R. Hu, Phys. Rev. Lett. **72**, 1526 (1994).
 - [3] K. Sengupta, H.-J. Kwon, and V. M. Yakovenko, cond-mat/0106198.
 - [4] TMTSF stands for tetramethyltetraselenafulvalene, X for inorganic anions such as PF₆ and AsF₆, and TMTTF for tetramethyltetrafulvalene.
 - [5] K. Sengupta, I. Žutić, H.-J. Kwon, V. M. Yakovenko, and S. Das Sarma, Phys. Rev. B **63**, 144531 (2001).
 - [6] K. Sengupta, H.-J. Kwon and V. M. Yakovenko, Phys. Rev. Lett. **86**, 1094 (2001).
 - [7] Yu. A. Firsov, V. N. Prigorin, and Chr. Seidel, Physics Reports **126**, 245 (1985).
 - [8] M. Fabrizio and A. O. Gogolin, Phys. Rev. B **51**, 17827 (1995).
 - [9] A. O. Gogolin, Phys. Rev. B **54**, 16063 (1996); K. Le Hur, Europhys. Lett. **49**, 768 (2000).
 - [10] T. Ishiguro, K. Yamaji, and G. Saito, *Organic Superconductors* (Springer, Berlin, 1998).
 - [11] F. Nad, P. Monceau, C. Carcel, and J. M. Fabre, J. Phys. Cond. Matt. **12**, L435 (2000); D. S. Chow *et al.*, Phys. Rev. Lett. **85**, 1698 (2000); P. Monceau, F. Ya. Nad, and S. Brazovskii, Phys. Rev. Lett. **86**, 4080 (2001).
 - [12] S. A. Brazovskii, Zh. Eksp. Teor. Fiz. **78**, 677 (1980) [Sov. Phys. JETP **51**, 342 (1980)]; S. A. Brazovskii, N. N. Kirova, and S. I. Matveenko, Zh. Eksp. Teor. Fiz. **86**, 743 (1984) [Sov. Phys. JETP **59**, 434 (1984)].
 - [13] A. Luther and V. J. Emery, Phys. Rev. Lett. **33**, 589 (1974).